



Early atmospheric contamination on the top of the Himalayas since the onset of the European Industrial Revolution

Paolo Gabrielli^{a,b,1}, Anna Wegner^a, M. Roxana Sierra-Hernández^a, Emilie Beaudon^a, Mary Davis^a, Joel D. Barker^{a,b}, and Lonnie G. Thompson^{a,b} 

^aByrd Polar and Climate Research Center, The Ohio State University, Columbus, OH 43210; and ^bSchool of Earth Sciences, The Ohio State University, Columbus, OH 43210

Edited by Mark H. Thiemens, University of California San Diego, La Jolla, CA, and approved January 3, 2020 (received for review June 19, 2019)

Because few ice core records from the Himalayas exist, understanding of the onset and timing of the human impact on the atmosphere of the “roof of the world” remains poorly constrained. We report a continuous 500-y trace metal ice core record from the Dasuopu glacier (7,200 m, central Himalayas), the highest drilling site on Earth. We show that an early contamination from toxic trace metals, particularly Cd, Cr, Mo, Ni, Sb, and Zn, emerged at high elevation in the Himalayas at the onset of the European Industrial Revolution (~1780 AD). This was amplified by the intensification of the snow accumulation (+50% at Dasuopu) likely linked to the meridional displacement of the winter westerlies from 1810 until 1880 AD. During this period, the flux and crustal enrichment factors of the toxic trace metals were augmented by factors of 2 to 4 and 2 to 6, respectively. We suggest this contamination was the consequence of the long-range transport and wet deposition of fly ash from the combustion of coal (likely from Western Europe where it was almost entirely produced and used during the 19th century) with a possible contribution from the synchronous increase in biomass burning emissions from deforestation in the Northern Hemisphere. The snow accumulation decreased and dry winters were reestablished in Dasuopu after 1880 AD when lower than expected toxic metal levels were recorded. This indicates that contamination on the top of the Himalayas depended primarily on multidecadal changes in atmospheric circulation and secondarily on variations in emission sources during the last 200 y.

ice cores | trace metals | paleoenvironment | monsoon | North Atlantic Oscillation

The timing of the first human impact on the Earth’s atmosphere varies spatially over the planet (1–3) and represents a key piece of information to establish the natural background of many chemical species and to specify the concept of the Anthropocene (4). The global population started to dramatically increase during the 18th century with a progressive impact on the environment including large-scale deforestation, particularly in Eurasia and Africa, to expand cropland and grassland areas (5). The Industrial Revolution started in Europe around 1780 AD and is a milestone of exceptional importance to evaluate the human impact on the global climate system (6). This period was characterized by the advent of machines, the introduction of engines to convert heat into work, and the rise of mineral power, particularly in the form of coal, to replace other energy sources (7).

During the 19th century, most of the coal power was produced in the United Kingdom, where most of the European and global coal was mined (8, 9). In this country, 70 to 90% of the internal coal consumption was destined for residential use, manufacturing, and iron and steel production (10). Coal-powered steam engines accounted for 20% of the power used in Britain by 1800 AD, and increased to 47% by 1830, 90% by 1870, and 98% by 1907 (11). By the 1840s, contemporary writers such as Engels (12) described cities blackened with thick smoke and urban slums crowded with diseased and dying people.

The United Kingdom exported a minor but increasing fraction of its total production over the 19th century (e.g., ~2% in 1822; ~20% in 1900 AD) (8). Eventually, coal-based technologies expanded to the rest of Europe and by the middle of the 19th century both coke-smelting and steam engines were also used in all of the coalfields of northern France, Belgium, and western Germany (13), diffusing emissions from coal combustion across Western Europe that likely became the most widespread source of atmospheric pollution at that time.

In addition to pollution from coal combustion, since the end of the 18th/beginning of the 19th centuries biomass burning emissions were linked to large-scale deforestation associated with land use change (5), which likely increased in the Northern Hemisphere as suggested by a compilation of sediment (14) and ice core records (15). However, the timing and magnitude of changes in past biomass burning emissions remain highly uncertain (16).

Coal and biomass combustion release various pollutants into the atmosphere, including soot particles, sulfur dioxide, and carbon dioxide. An important component of these emissions is the fine fraction of soot (fly ash), which is enriched in trace metals (17). Coal fly ash is characterized by Ba, Bi, Co, Cr, Cs, Mo, Ni, and, particularly, As, Cd, Ga, Pb, Sb, Ti, and Zn (18), the emission factors of which are significant (19). When compared to

Significance

Since the beginning of the European Industrial Revolution (~1780 AD), increases in the deposition of atmospheric toxic metals were recorded in an ice core extracted from the Dasuopu glacier, at very high elevation (7,200 m) in the Himalayas. Initially, these contaminants were transported by the winter westerlies as combustion products of coal, likely used in Europe, during the 19th century, with the possible contribution from the emissions of large-scale fires used for deforestation. During the 20th century, unexpected low levels of toxic metals suggest that multidecadal changes in atmospheric circulation are the most important factor to explain the impact of human emissions on the chemistry of the troposphere in the Himalayas at this time.

Author contributions: P.G. and L.G.T. designed research; P.G., A.W., M.R.S.-H., and E.B. performed research; P.G., A.W., M.R.S.-H., E.B., M.D., and J.D.B. analyzed data; and P.G., A.W., and J.D.B. wrote the paper.

The authors declare no competing interest.

This article is a PNAS Direct Submission.

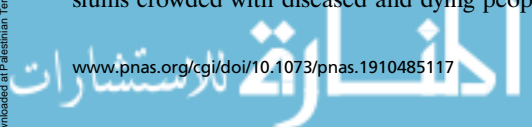
Published under the PNAS license.

Data deposition: The data presented in this work have been archived at the National Oceanic and Atmospheric Administration World Data Center, <https://www.ncdc.noaa.gov/> (Study ID 28510).

¹To whom correspondence may be addressed. Email: gabrielli.1@osu.edu.

This article contains supporting information online at <https://www.pnas.org/lookup/suppl/doi:10.1073/pnas.1910485117/-DCSupplemental>.

First published February 10, 2020.



coal, biomass ash is typically less enriched in trace metals with some notable exceptions, such as Mg (5 times more enriched), Mn (8), Rb (13), and Zn (7) (from ref. 20). Fly ash particles have an atmospheric residence of up to 10 d (21), and when deposited their elemental composition can be used in paleoenvironmental archives as a fingerprint of deposition of coal and biomass combustion products of atmospheric origin (22).

Ice cores provide striking evidence of past atmospheric contamination linked to the rise and development of anthropogenic activities by ancient civilizations in various continents during human history. For instance, toxic trace metals emitted from mining and metallurgical operations conducted in Western Europe by the Romans (Spain, 200 AD), in South America by the Spaniards (Bolivia, 1570 AD), and in Australia by the colonial population (Broken Hills, 1889 AD) were transported over long ranges and contaminated the atmosphere and the snow in central Greenland and Antarctica with Pb (3, 23), and in South America with As, Bi, Cu, Mo, Pb, and Sb (24, 25).

In Asia, evidence of past atmospheric contamination is restricted to ice cores that record the first anthropogenic deposition beginning in the 20th century, when increases in contamination of the atmosphere and deposition of long-range transported trace metals from various anthropogenic sources are clearly documented on the glaciers of Altai (26–28), the Tibetan Plateau (29, 30), and the Himalayas (31, 32). However, a more recent trace metal ice core record from the Guliya ice cap in Western Tibet suggests an earlier anthropogenic fallout in Central Asia, perhaps linked to the transport and deposition of coal combustion products from Western Europe beginning during the 19th century (22). Unfortunately, the high dust background in the Guliya core prevents the unequivocal identification of the onset and origin of atmospheric anthropogenic contamination in Asia during the early industrial period.

So far, only trace metal records from polar ice cores have been considered sufficiently remote from anthropogenic sources to be of hemispheric significance (3, 33). Conversely, low-latitude/high-altitude ice core records have been demonstrated to typically record atmospheric contributions of regional origin (24, 26, 29, 34), mainly because of their proximity to natural (crustal) and anthropogenic sources of atmospheric trace metals.

The Dasuopu ice core was drilled in 1997 at 7,200-m altitude in the central Himalayas (28°23'N; 85°43'E) (Fig. 1), and it

provides the highest elevation climate record yet obtained (35). This site is normally heavily influenced by the monsoon regime that causes a strong seasonal cycle in the snow accumulation rate (~1,000 mm water equivalents [w.e.] per y). Due to the very high altitude and relief over the surrounding terrain, Dasuopu is characterized by a very low aeolian dust background (35). Therefore, this low-latitude/high-altitude site is potentially well suited to archive not only atmospheric contaminants of regional significance, but also long-traveled chemical constituents from the whole of the Northern Hemisphere.

Notably, the excellent preservation of annual layers in the Dasuopu core allows the reconstruction of a very detailed record of past snow accumulation (35) (Fig. 2). This is rare information among low-latitude/high-altitude ice cores and can be used to compute a unique record of the atmospheric chemical fluxes to the central Himalayas. By studying intraannual and decadal variations of trace element concentrations, their fluxes and their crustal enrichment factors (EFs) (*SI Appendix, Text S4*), we focus this paper on the detection of the onset, origin, and development of atmospheric contamination from anthropogenic trace metals at a very high altitude in the Himalayas, with particular attention on the early industrial period of the 19th century.

Results and Discussion

We present records for the concentrations of 23 trace metals (Al, As, Ba, Bi, Cd, Co, Cr, Cs, Fe, Ga, Mg, Mn, Mo, Nb, Ni, Pb, Rb, Sb, Ti, Tl, U, V, and Zn) determined in the C3 Dasuopu ice core (see *Methods*) over the time interval 1499 to 1992 AD. Trace metal concentrations (Fig. 2 and *SI Appendix, Figs. S1 and S2 and Table S1*) are extremely variable in the Dasuopu core, with values ranging from 100 ng·g⁻¹ for typical crustal elements, such as Al and Fe, to picogram-gram⁻¹ and subpicogram-gram⁻¹ levels for ultra-trace metals such as, Cr, Sb, Tl, Pb, and Bi, which are comparable to concentrations found in the Arctic snow and ice (33, 36, 37).

The annual/seasonal variability of trace metal concentrations is well recorded and very high, typically two orders of magnitude, with peak crustal elements concentrations occurring during the winter to spring months (*SI Appendix, Figs. S3–S5*). Concentration variability is much lower from 1499 to ~1700 AD, because of diffusion due to the thinning of ice layers at greater englacial depths. Notably, as illustrated by the decadal median trends, most of the trace metal concentrations show a significant wide minimum during the 19th century (Fig. 2 and *SI Appendix, Figs.*

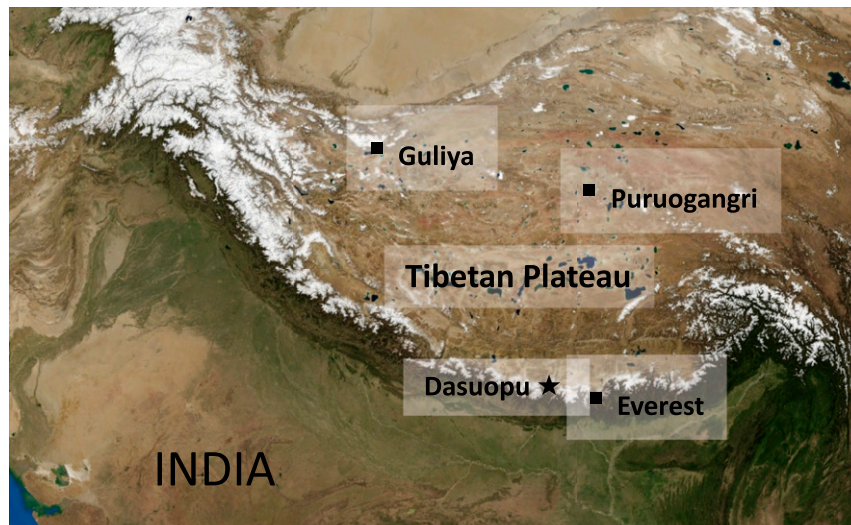


Fig. 1. Location and study site. The Dasuopu ice core drilling site in the Himalayas (marked by a star) and other significant locations mentioned in the text are shown. Map courtesy of Wikimedia Commons/NASA.

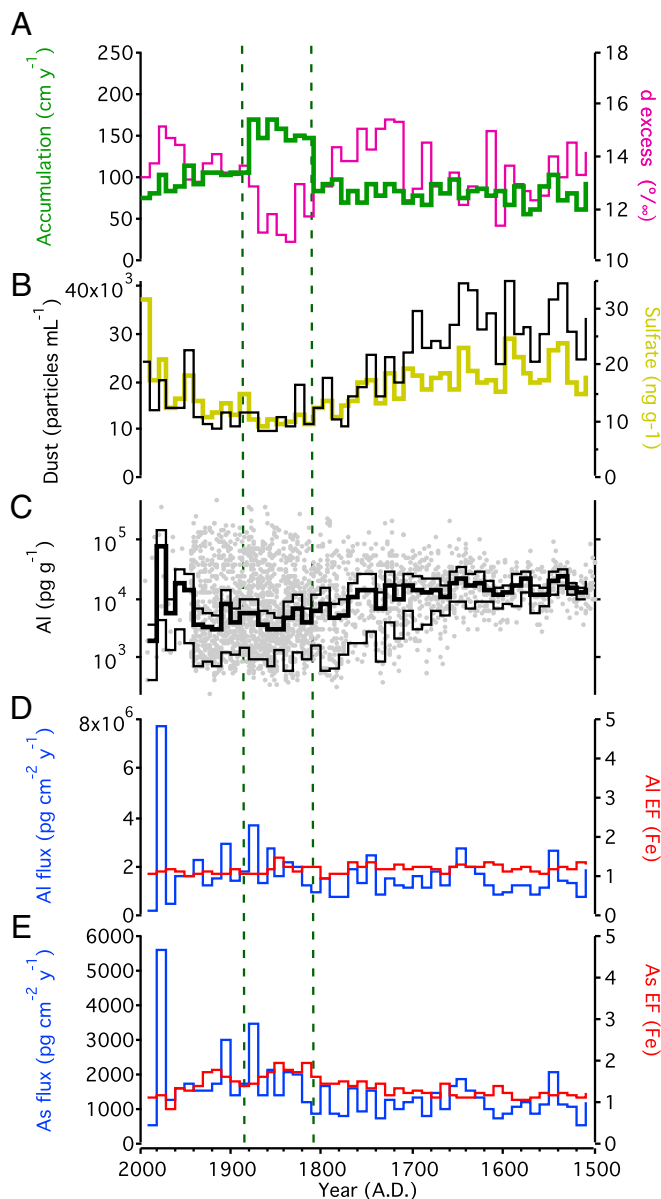


Fig. 2. Climatic and geochemical parameters in the Dasuopu ice core, all shown as decadal medians. From the *Top*: (A) snow accumulation and deuterium excess (35); (B) dust particle and sulfate concentrations (35, 38); (C) Al concentration (gray dots represent single sample values; cityscape curves depict decadal median [in bold] bracketed by median absolute deviation); (D and E) Al, As fluxes and crustal EFs. The vertical dotted lines outline the 1810 to 1880 AD period with high snow accumulation.

S1 and S2). Importantly, a corresponding wide minimum can also be observed in the Dasuopu core in the decadal median of different proxies other than trace metals, such as for instance dust particles (35) and sulfate (38) (Fig. 2).

In this context, an increase in snow accumulation rate (from ~ 100 to ~ 150 cm w.e. per y) and a concomitant minimum in deuterium excess are observed between 1810 and 1880 AD (Fig. 2). It is important to note that the synchronous variation in snow accumulation and deuterium excess rules out glacial dynamic postdepositional effects (e.g., significant horizontal flow altering the snow layers). We note that the observed decreases in trace metal concentrations (e.g., Al and As) are compensated for by the increase in snow accumulation such that the calculated fluxes (e.g., Al concentration \times snow accumulation; Fig. 2) show

limited variability over the entire 500-y ice core record (*SI Appendix, Table S2*), with the exception of the 1970 to 1980 decade, when high crustal species are recorded. We conclude that the broad 19th-century minimum for most trace metal concentrations was mainly caused by the 50% increase in snow accumulation that diluted the dominant dry fallout of the chemical species.

Arsenic (As) is a trace element that is well known to be widely enriched in Tibetan Plateau soil dust (39) and occasionally also in central India rocks (40). We use the elemental composition of soil dust collected from Tibet as a crustal standard and Fe as crustal elemental reference to calculate EF (29). In this case, EFs of As and Al are rather constant and close to 1 through the entire 500-y record (Fig. 2), suggesting a constant origin of aeolian dust from the Tibetan Plateau and/or perhaps central India to the high altitudes of the Himalayas during the last 500 y. While it remains plausible that aeolian dust from sources such as the Arabian Peninsula, Thar Desert, and northern Sahara occasionally travel to the central Himalayan region (41), we suggest that the regional sources have been the prevalent dust provenance for Dasuopu during the last 500 y. Interestingly, during the 19th century, an $R^2 = 0.45$ ($R^2 = 0.59$ by removing the four largest outliers) between Ca^{2+} and SO_4^{2-} (35) suggests that a contribution from evaporitic minerals of sedimentary origin (gypsum, CaSO_4) may have strongly imprinted the low sulfate background.

The EFs of other typical crustal elements (Ba, Cs, Mg, Ti, U, and V) also remain constant through time (*SI Appendix, Table S3*), with median decadal values at or near 1.0 (but below 1.2) concomitant with relative increases in their fluxes (40 to 80%) since the beginning of the 19th century (*SI Appendix, Table S2*). In contrast, EFs of other trace metals (Bi, Cd, Cr, Mo, Ni, Sb, Tl, and Zn) show increases at the end of the 18th century, with median decadal values between 1.7 (Bi) and 5.4 (Zn) (Fig. 3 and *SI Appendix, Fig. S7*), concomitant with larger increase of their fluxes (70 to 330%).

We note that, unlike trace metal concentrations, variations in EF are independent of changes in snow accumulation (and thus fluxes) and need to be explained in terms of variations of the emission sources and/or transport (atmospheric circulation). When combined, these observations suggest that an additional noncrustal fraction of trace metals, such as Bi, Cd, Cr, Mo, Ni, Sb, Tl, and Zn, was transported to high altitude in the central Himalayas since the end of the 18th century (Fig. 3 and *SI Appendix, Fig. S7*). The amplitude and the peculiar persistence of these metal enrichments over time point to diffused anthropogenic sources as the likely contributor of this noncrustal fraction of trace elements.

To assess the sources of this change in the atmospheric chemistry of the central Himalaya, positive matrix factorization (PMF) was applied to the concentration dataset (*SI Appendix, Text S1*). Factors 2 and 3 may highlight the distant and regional contributions from the geological background, respectively, because 1) the generally low EF values and limited variability for their characteristic trace metals; 2) the negligible (1%) and high (66%) distribution of arsenic (the proxy of regional crustal background) on these two factors (*SI Appendix, Table S4*). In contrast, factor 1 is likely linked to anthropogenic activities as it shows a well-defined group of several trace elements that also have notable increases in EF, primarily Cd, Mo, Sb, Zn, and secondarily Cr and Ni (*SI Appendix, Table S4*). Interestingly, PMF also demonstrates that anthropogenic Pb mass concentration is lower than its crustal contribution by a factor of 4 (*SI Appendix, Table S5*).

The temporal trend of the anthropic factor 1 (Fig. 4) shows an initial increase at the end of the 18th/beginning of the 19th centuries that parallels European coal production (9) and charcoal deposition from biomass burning in the Northern Hemisphere (14). A further progressive increase of the anthropic

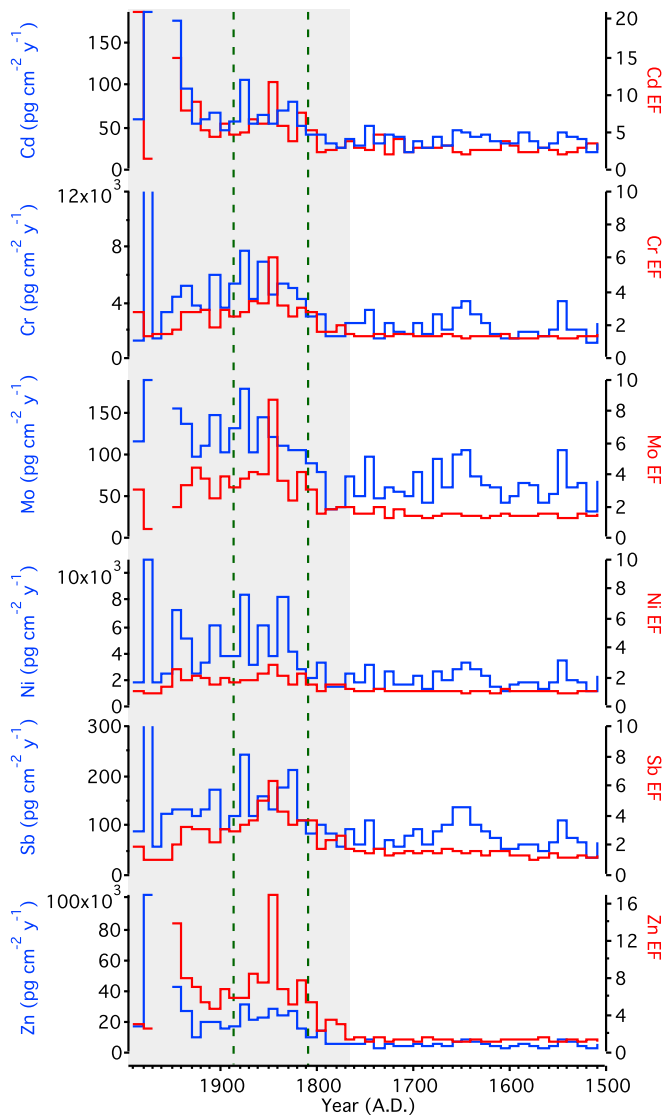


Fig. 3. Chemical fluxes and crustal EFs (decadal medians) of Cd, Cr, Mo, Ni, Sb, and Zn that show the largest variations in the Dasuopu ice core during the last 500 y. The vertical dotted lines outline the 1810 to 1880 AD period with high snow accumulation, while the gray band spans the period of anthropogenic contributions.

factor 1 is observed during the 20th century, peaking in the 1940s to 1950s, and even more remarkably in the 1970s to 1980s. Interestingly, the crustal PMF factors 2 and 3 also peak during the second half of the 20th century (*SI Appendix, Fig. S8*), indicating an increase in the input of crustal dust to the Dasuopu glacier [see also Al (Fig. 2) and Fe (*SI Appendix, Fig. S10*) concentrations]. In this case, the recent increase in flux of elements such as Fe, Co, and U (*SI Appendix, Fig. S7*) may be explained with the augmented deflation of regional dust from expanded soils used for agriculture and pasture (5).

The European Industrial Revolution started a few decades earlier than the beginning of the period marked by change in snow accumulation and deuterium excess observed in the Dasuopu core (1810 to 1880 AD) (Figs. 2 and 4). This hydroclimatic event seems of notable significance because it appears to have modulated the early advection and deposition of atmospheric contaminants to high elevation glaciers in the central Himalayas. This ~70-y climatic feature observed in the Dasuopu core has been previously described (42). Briefly, the large step

increase in snow accumulation was found to be significantly correlated ($R = 0.32$; 95% significance level) with the November and December Northern Atlantic Oscillation index (NAO) calculated from instrumental values (43) (Fig. 4). It was concluded that the 1810 to 1880 AD increase in snow accumulation on Dasuopu was linked to the intensification of precipitation, probably because of the meridional displacement of the winter

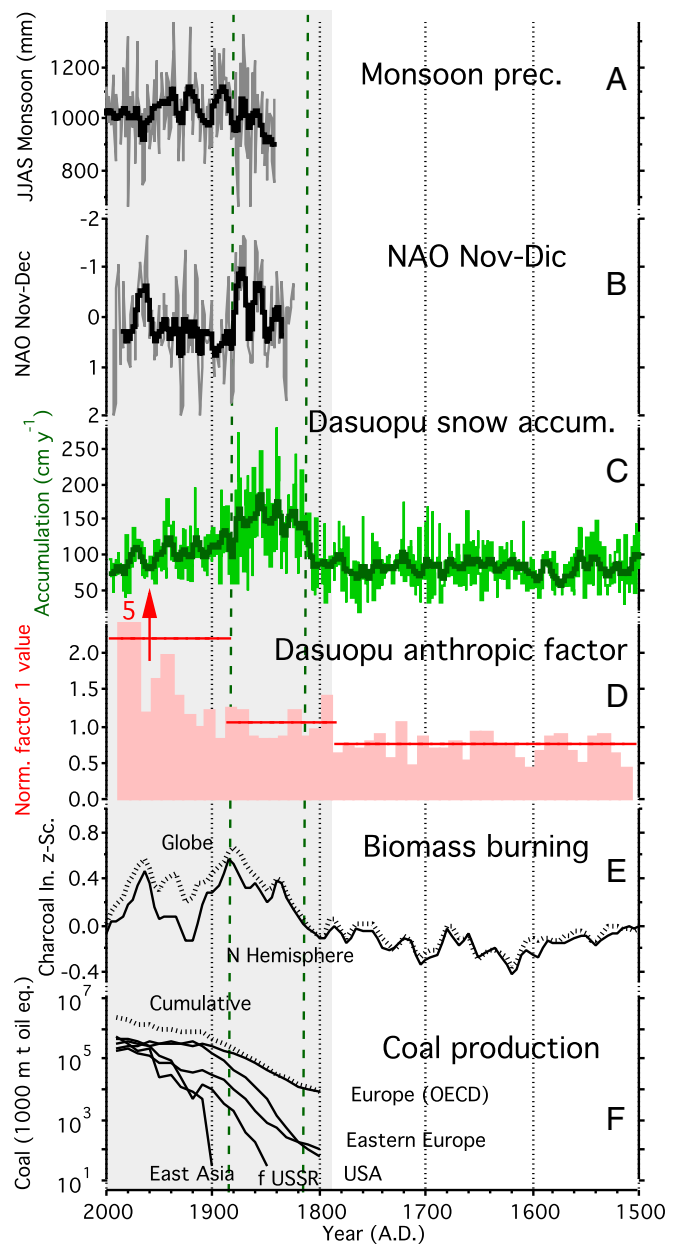


Fig. 4. Hydroclimatology, anthropic factor, biomass burning, and coal production. The annual records, overlain by 5-y median smoothing, of the following: (A) monsoon summer (June to September [JJAS]) precipitation in India (46), (B) November to December North Atlantic Oscillation Index (NAO) (42), and (C) Dasuopu snow accumulation (35). (D) Decadal median of the anthropic factor 1 (Zn, Mo, Cd, Sb) from positive matrix factorization (PMF) of the trace metal concentration dataset of the Dasuopu ice core and (E) charcoal influx z score in the globe and in the Northern Hemisphere (14). (F) Cumulative global and regional coal production since 1800 AD (9). The vertical dotted lines outline the 1810 to 1880 AD period with high snow accumulation, while the gray band spans the period of anthropogenic contributions to trace metal deposition in Dasuopu.

westerlies under negative NAO conditions (44). While an increase in deuterium excess can be expected from modern moisture transported by the westerlies to Dasuopu (45), the opposite pronounced decrease observed during the 1810 to 1880 AD period (Fig. 2) is consistent with the contribution of humid air masses from the Tropical Indian Ocean (45) that might have been intercepted by the relocated southern flow of the westerlies at that time. Incorporation of tropical moisture in the western flow would also better explain the remarkable increase in snow accumulation recorded in Dasuopu during the 19th century.

The proposed meridional displacement of the westerlies is supported by the observation of a concomitant extended drought north of the central Himalayas (Puruogangri, central Tibetan plateau) during the 19th century (29). The lack of significant correlation between the Dasuopu snow accumulation and summer monsoon precipitation in Central Northern India (46) ($R = 0.05$) before 1880 AD further corroborates this interpretation. After 1880 AD, the correlation between snow accumulation and the NAO index becomes insignificant, while the correlation between accumulation and summer monsoon precipitation becomes significant ($R = 0.43$; 95% significance level), respectively (42). This suggests that the typical seasonal precipitation pattern was established in the central Himalayas after 1880 AD (Fig. 4).

The intensification in the winter snow accumulation during the 1810 to 1880 AD period is paralleled by anomalous patterns in the seasonal deposition of noncrustal trace metals. During the 20th century, EF typically shows low values during the dry winter/spring season and higher levels during the wet summer monsoon (*SI Appendix*, Fig. S3). This is opposite to the seasonal variations of $\delta^{18}\text{O}$, dust, and trace element concentrations, as typically observed in high-altitude sites that are characterized by a strong seasonality in snow accumulation (47). During the 19th century, despite the marked perseverance of the seasonal patterns of stable isotopes, dust, and crustal element concentrations, the variations of EF of typical noncrustal elements (e.g., Sb, Zn, and Mo) become less obviously seasonal with frequent high values also during winter (*SI Appendix*, Fig. S4; comparison between the two periods in *SI Appendix*, Fig. S6). This suggests that the observed increase in EF during the 19th century (Fig. 3) was caused by an additional noncrustal fraction, which was mainly deposited during the anomalously wet winters.

We used modern (1948 to 1992) atmospheric back trajectories to explore potential source areas of the trace metal contaminants in the Dasuopu glacier (*SI Appendix*, Fig. S13). While 7-d atmospheric summer back trajectories display a frequency field extending to India, the Arabian Sea, and the Middle East, winter back trajectories extend as far as North Africa, Central Europe, and the North Atlantic, suggesting a western origin for the additional metals of noncrustal origin deposited in winter during the 1810 to 1880 AD period. Hereafter, we show that the higher EF and the statistical linkage between Cd, Cr, Mo, Ni, Sb, and Zn (PMF anthropic factor 1), all enriched due to emissions from coal and biomass combustion (18, 48), point to the scenario in which they were transported from widely diffused sources of atmospheric pollution in Western Europe for coal combustion with a possible contribution from forest fires during the 19th century.

European economic data such as coal production and import/export records are available only since the early 19th century (8), during which nearly the entire world's supply of coal was produced and probably combusted in Western Europe (9) (Fig. 4). It is likely that Western Europe became the most important global emitter of coal ash during the 19th century. Data about coal production in Asia exist only since 1874 AD and show that in India and China it was only 1 to 2% of European production, even by the end of the 19th century (8). As far as is known, there are no data on coal imports in India and China at this time. In any event, these imports were likely to have been negligible because of the very low level or absence of industrialization in these

two countries during this period (49, 50), implying negligible regional emissions from coal combustion and other activities such as mining operations in India and China during the 19th century.

At that time, while local emissions from coal combustion are unlikely to have significantly impacted the atmosphere of the central Himalayas, we cannot rule out that trace metals originating from regional and hemispheric-scale biomass burning impacted the chemistry of the Dasuopu glacier. Relatively high EF of Zn (Fig. 3) and Zn mass ratios are consistent with the deposition of a mixture of coal and biomass ashes (*SI Appendix*, Fig. S9 and Text S3). As far as we know, while there are no specific data for India and China that extend back to the 18th century, it is documented that South Asia underwent an intense change in land use with a 0.6% per year increase of cropland area (net absolute change, 43 Mha in the 18th century), similar to the former USSR (0.7% per year; 33 Mha) and Western Europe (0.3% per year; 19 Mha) (5). These increases may have been correlated to diffuse deforestation by means of biomass burning since the 18th century.

The Dasuopu record after 1880 AD shows that moisture-bearing winter westerlies weakened, trace metal concentrations increased, while anthropogenic trace elements fluxes (Cd, Cr, Mo, Ni, Sb and Zn; Fig. 3) remained at a rather constant level above the preindustrial background. EFs slightly decreased until 1950, although still remaining well above background levels (Fig. 3 and *SI Appendix*, Fig. S1 and Tables S1–S3). These observations suggest that the increase in concentrations observed in the Dasuopu ice core after 1880 AD could have been due not only to the decrease in snow accumulation rate, but also to a stronger increase in trace metal atmospheric levels, perhaps related to biomass burning emissions due to wildfires linked to the more frequent droughts that occurred in India since the end of the 19th century (51, 52).

In light of the observed trends in trace metal deposition between the 19th century and the first half of the 20th century, we suggest that variations in snow accumulation rate and the sources of moisture at high elevation in the central Himalayas played major roles in determining concentrations, fluxes, and EF levels in the Dasuopu core during this period. Overall, this indicates that, at decadal timescales, the impact of the atmospheric contaminants to the highest Himalayan glaciers can be governed primarily by variations in atmospheric circulation, and secondarily by changes in emission from anthropogenic sources.

No large EF increase is observed in the second half of the 20th century for most of the trace metals, including typical anthropogenic tracers such as Bi, Cd, Cr, Sb, V, and Zn (*SI Appendix*, Table S3), in part because of the synchronous increase in crustal dust concentration as suggested by PMF factors 2 to 3 and Fe concentrations (*SI Appendix*, Figs. S8 and S10). The only exception is Pb, the concentration, flux, and EF of which appear to have increased by an order of magnitude, a factor of 2, and 50%, respectively (*SI Appendix*, Figs. S2, S7, and S11). This is in line with a parallel increase in Pb concentrations determined after 1950 in another firn core from Dasuopu (53), and the observed increase of Pb in other ice core records from the Tibetan Plateau, Himalayas, and Alaska (22, 29, 54–56) that were linked to intensified Pb emissions from gasoline combustion (57). However, the lower-than-expected trace metal levels during this more recent interval (1950 to 1992 AD) in Dasuopu could be also linked to the fact that it was only possible to discretely sample and analyze ~15% of the recent firn portion of the Dasuopu core covering 1950 to 1992 AD (*SI Appendix*, Text S4); we cannot entirely rule out the possibility that our analysis did not completely capture the trace metal variability over this selected time period.

In conclusion, this study places onset of anthropogenic contamination of the atmosphere and the pristine snow of the

central Himalayas at the end of the 18th/beginning of the 19th centuries, in close concomitance with the start of the European Industrial Revolution, the increasing emissions from coal combustion, and regional/hemispheric biomass burning, likely from deforestation practices. At that time, Dasuopu, and most likely the central Himalayas as a whole, were probably affected by the fallout of fine fly ash transported by anomalous winter west-erlies and deposited with the winter snow. This peculiar atmospheric circulation was likely the key factor that allowed the onset of human contamination at very high altitudes in the central Himalayas.

Methods

The Dasuopu C3 ice core was used in this work (35). It was extracted in 1997 and stored in the freezers at The Ohio State University for more than two decades. As described in ref. 35, an annual record was reconstructed during the last 560 y through the distinct seasonal cycles in $\delta^{18}\text{O}$, dust, and NO_3^- . The annual layer counting was confirmed at 42.2 m by the location of the 1963 beta radioactivity signature from the 1962 atmospheric thermonuclear tests. Based on the dust and $\delta^{18}\text{O}$ stratigraphy, the ice core C3 was annually dated to 1440 AD with an uncertainty of 3 y at 145.4-m depth.

We processed a total of 2,564 core samples down to 143-m depth (corresponding to 1499 AD). The upper 55-m section covers the time interval from 1950 to 1992 AD and consists of firn discontinuously sampled in 29 sections of ~20- to 30-cm length, each encompassing less than 1 y of accumulation. Between 55- and 143-m depth, the core is composed of ice and spans 1499 to 1950 AD. This was continuously sampled at subannual resolution (at least seven samples per y) from 55 to 121 m (1775 AD; 10- to 2.5-cm sample

intervals) and with lower resolution between 121 and 143 m (1499 AD; constant 2.5-cm intervals).

Analyses of 23 trace elements (Al, As, Ba, Bi, Cd, Co, Cr, Cs, Fe, Ga, Mg, Mn, Mo, Nb, Ni, Pb, Rb, Sb, Ti, Tl, U, V, and Zn) were performed at the Byrd Polar and Climate Research Center (BPCRC) of The Ohio State University by inductively coupled plasma sector field mass spectrometry (ICP-SFMS; Thermo, Element2). Accuracy, precision, and blanks were consistent with those previously published by our laboratory (22, 29, 58). Additional information about the methods are provided in *SI Appendix, Text S4*.

Data Deposition. The data presented in this work have been archived at the National Oceanic and Atmospheric Administration (NOAA) World Data Center A for Paleoclimatology: <https://www.ncdc.noaa.gov/paleo/study/28510> (59).

ACKNOWLEDGMENTS. This work was funded by the NSF Atmospheric Chemistry Program (Award 1149239), the NSF-Earth System History Program, The Ohio State University, the Ohio State Committee of Science and Technology, and the National Natural Science Foundation of China. The mass spectrometer (ICP-SFMS) at the BPCRC was funded by NSF-Major Research Instrumentation Award 0820779 and by the Climate Water Carbon Program of The Ohio State University. We thank the many scientists, engineers, technicians, and graduate students from the BPCRC and the Lanzhou Institute of Glaciology and Geocryology (China). We also thank Jacopo Gabrieli and Carlo Barbante at the University of Venice for providing the lathe that allowed us to process the firn sections. We are also grateful to Julien Nicolas for performing the graphic display of the back trajectories and Susan Kaspari for providing trace metal data from the Mount Everest ice core. Finally, we thank two anonymous reviewers for providing constructive comments that allowed us to remarkably improve the initial manuscript. This is BPCRC Contribution No. C-1591.

1. S. Hong, J. P. Candelone, C. C. Patterson, C. F. Boutron, Greenland ice evidence of hemispheric lead pollution two millennia ago by Greek and Roman civilizations. *Science* **265**, 1841–1843 (1994).
2. A. Eichler *et al.*, Ice-core evidence of earliest extensive copper metallurgy in the Andes 2700 years ago. *Sci. Rep.* **7**, 41855 (2017).
3. J. R. McConnell *et al.*, Antarctic-wide array of high-resolution ice core records reveals pervasive lead pollution began in 1889 and persists today. *Sci. Rep.* **4**, 5848 (2014).
4. P. J. Crutzen, E. F. Stoermer, The “Anthropocene.” *Global Change Newsl.* **41**, 17–18 (2000).
5. K. K. Goldewijk, G. Van Dreht, “HYDE 3: Current and historical population and land cover” in *Integrated Modelling of Global Environmental Change: An Overview of IMAGE 2.4*, A. F. Bouwman, T. Kram, K. K. Goldewijk, Eds. (Netherlands Environmental Assessment Agency, Bilthoven, 2006), pp. 93–112.
6. N. J. Abram *et al.*, PAGES 2k Consortium, Early onset of industrial-era warming across the oceans and continents. *Nature* **536**, 411–418 (2016).
7. D. S. Landes, *The Rise of Capitalism* (Macmillian, New York, 1966).
8. B. R. Mitchell, *International Historical Statistics: Europe, 1750–1993* (MacMillian Reference Ltd, London, 1998).
9. HYDE, History database of the global environment. <https://themasites.pbl.nl/tridion/en/themasites/hyde/index.html>. Accessed 20 October 2019.
10. B. R. Mitchell, *British Historical Statistics* (Cambridge University Press, Cambridge, UK, 1988).
11. N. Crafts, Steam as a general purpose technology: A growth accounting perspective. *Econ. J. (Lond.)* **114**, 338–351 (2004).
12. F. Engels, *The Condition of the Working Class in England* (Penguin Books, 1845).
13. E. A. Wrigley, *Industrial Growth and Population Change; A Regional Study of the Coalfield Areas of North-West Europe in the Later Nineteenth Century* (Cambridge University Press, Cambridge, UK, 1961).
14. J. R. Marlon *et al.*, Reconstructions of biomass burning from sediment-charcoal records to improve data–model comparisons. *Biogeosciences* **13**, 3225–3244 (2016).
15. M. Legrand *et al.*, Boreal fire records in Northern Hemisphere ice cores: A review. *Clim. Past* **12**, 2033–2059 (2016).
16. M. J. E. van Marle *et al.*, Historic global biomass burning emissions for CMIP6 (BB4CMIP) based on merging satellite observations with proxies and fire models (1750–2015). *Geosci. Model Dev.* **10**, 3329–3357 (2017).
17. A. B. Ross *et al.*, Measurement and prediction of the emission of pollutants from the combustion of coal and biomass in a fixed bed furnace. *Fuel* **81**, 571–582 (2002).
18. M. Xu *et al.*, Status of trace element emission in a coal combustion process: A review. *Fuel Process. Technol.* **85**, 215–237 (2004).
19. M. S. Reddy, S. Basha, H. V. Joshi, B. Jha, Evaluation of the emission characteristics of trace metals from coal and fuel oil fired power plants and their fate during combustion. *J. Hazard. Mater.* **123**, 242–249 (2005).
20. S. V. Vassilev, C. G. Vassileva, D. Baxter, Trace element concentrations and associations in some biomass ashes. *Fuel* **129**, 292–313 (2014).
21. S. K. Marx, H. A. McGowan, “Long-distance transport of urban and industrial metals and their incorporation into the environment: Sources, transport pathways and historical trends” in *Urban Airborne Particulate Matter*, F. Zereini, C. Wiseman, Eds. (Springer, Berlin, 2010).
22. M. R. Sierra Hernandez, P. Gabrielli, E. Beaudon, A. Wegner, L. G. Thompson, Atmospheric depositions of natural and anthropogenic trace elements on the Guliya ice cap (northwestern Tibetan Plateau) during the last 340 years. *Atmos. Environ.* **176**, 91–102 (2018).
23. J. R. McConnell *et al.*, Lead pollution recorded in Greenland ice indicates European emissions tracked plagues, wars, and imperial expansion during antiquity. *Proc. Natl. Acad. Sci. U.S.A.* **115**, 5726–5731 (2018).
24. C. Uglietti, P. Gabrielli, C. A. Cooke, P. Vallelonga, L. G. Thompson, Widespread pollution of the South American atmosphere predates the Industrial Revolution by 240 y. *Proc. Natl. Acad. Sci. U.S.A.* **112**, 2349–2354 (2015).
25. A. Eichler, G. Gramlich, T. Kellerhals, L. Tobler, M. Schwikowski, Pb pollution from leaded gasoline in South America in the context of a 2000-year metallurgical history. *Sci. Adv.* **1**, e1400196 (2015).
26. A. Eichler *et al.*, Three centuries of Eastern European and Altai lead emissions recorded in a Belukha ice core. *Environ. Sci. Technol.* **46**, 4323–4330 (2012).
27. A. Eichler *et al.*, Ice-core based assessment of historical anthropogenic heavy metal (Cd, Cu, Sb, Zn) emissions in the Soviet Union. *Environ. Sci. Technol.* **48**, 2635–2642 (2014).
28. S. Eyrikh *et al.*, A 320 year ice-core record of atmospheric Hg pollution in the Altai, Central Asia. *Environ. Sci. Technol.* **51**, 11597–11606 (2017).
29. E. Beaudon, P. Gabrielli, M. R. Sierra-Hernández, A. Wegner, L. G. Thompson, Central Tibetan Plateau atmospheric trace metals contamination: A 500-year record from the Puruogangri ice core. *Sci. Total Environ.* **601–602**, 1349–1363 (2017).
30. S. Kang *et al.*, Atmospheric mercury depositional chronology reconstructed from lake sediments and ice core in the Himalayas and Tibetan Plateau. *Environ. Sci. Technol.* **50**, 2859–2869 (2016).
31. S. Hong *et al.*, An 800-year record of atmospheric As, Mo, Sn, and Sb in central Asia in high-altitude ice cores from Mt. Qomolangma (Everest), Himalayas. *Environ. Sci. Technol.* **43**, 8060–8065 (2009).
32. S. Kaspari *et al.*, Recent increases in atmospheric concentrations of Bi, U, Cs, S and Ca from a 350-year Mount Everest ice core record. *J. Geophys. Res. Atmos.* **114**, D04302 (2009).
33. J. R. McConnell, R. Edwards, Coal burning leaves toxic heavy metal legacy in the Arctic. *Proc. Natl. Acad. Sci. U.S.A.* **105**, 12140–12144 (2008).
34. J. Gabrieli, C. Barbante, The Alps in the age of the Anthropocene: The impact of human activities on the cryosphere recorded in the Colle Gnifetti glacier. *Rend. Lincei* **25**, 71–83 (2014).
35. L. G. Thompson *et al.*, A high-resolution millennial record of the South Asian monsoon from Himalayan ice cores. *Science* **289**, 1916–1920 (2000).
36. M. Krachler, J. Zheng, D. Fisher, W. Shotyk, Atmospheric Sb in the Arctic during the past 16,000 years: Responses to climate change and human impacts. *Global Biogeochem. Cycles* **22**, GB1015 (2008).
37. M. Krachler, J. Zheng, D. Fisher, W. Shotyk, Global atmospheric As and Bi contamination preserved in 3000 year old Arctic ice. *Global Biogeochem. Cycles* **23**, GB3011 (2009).
38. K. Duan, L. G. Thompson, T. Yao, M. E. Davis, E. Mosley-Thompson, A 1000 year history of atmospheric sulfate concentrations in southern Asia as recorded by a Himalayan ice core. *Geophys. Res. Lett.* **34**, L01810 (2007).

39. C. Li, S. Kang, Q. Zhang, Elemental composition of Tibetan Plateau top soils and its effect on evaluating atmospheric pollution transport. *Environ. Pollut.* **157**, 2261–2265 (2009).
40. K. S. Patel *et al.*, Arsenic contamination in water, soil, sediment and rice of central India. *Environ. Geochem. Health* **27**, 131–145 (2005).
41. S. Kaspari *et al.*, A high-resolution record of atmospheric dust composition and variability since A.D. 1650 from a Mount Everest ice core. *J. Clim.* **22**, 3910–3925 (2009).
42. M. E. Davis, L. G. Thompson, T. Yao, N. Wang, Forcing of the Asian monsoon on the Tibetan Plateau: Evidence from high-resolution ice core and tropical coral records. *J. Geophys. Res. Atmos.* **110**, D04101 (2005).
43. P. D. Jones, T. Jonsson, D. Wheeler, Extension to the North Atlantic oscillation using early instrumental pressure observations from Gibraltar and south-west Iceland. *Int. J. Climatol.* **17**, 1433–1450 (1997).
44. J. G. Pinto, C. C. Raible, Past and recent changes in the North Atlantic oscillation. *Wiley Interdiscip. Rev. Clim. Change* **3**, 79–90 (2012).
45. L. Tian, Y. Tandong, J. W. C. White, W. Yu, N. Wang, Westerly moisture transport to the middle of Himalayas revealed from the high deuterium excess. *Chin. Sci. Bull.* **50**, 1026–1030 (2005).
46. N. A. Sontakke, N. Singh, H. N. Singh, Instrumental period rainfall series of the Indian region (AD 1813–2005): Revised reconstruction, update and analysis. *Holocene* **18**, 1055–1066 (2008).
47. J. Gabrieli *et al.*, Impact of Po' Valley emissions on the highest glacier of the Eastern European Alps. *Atmos. Chem. Phys.* **11**, 8087–8102 (2011).
48. C. A. Alves *et al.*, Smoke emissions from biomass burning in a Mediterranean shrubland. *Atmos. Environ.* **44**, 3024–3033 (2010).
49. D. Clingingsmith, J. G. Williamson, Deindustrialization in 18th and 19th century India: Mughal decline, climate shocks and British industrial ascent. *Explor. Econ. Hist.* **45**, 209–234 (2008).
50. D. H. Perkins, Government as an obstacle to industrialization: The case of nineteenth-century China. *J. Econ. Hist.* **27**, 478–492 (1967).
51. D. A. Mooley, B. Parthasarathy, N. A. Sontakke, A. A. Munot, Annual rain-water over India, its variability and impact on the economy. *J. Clim.* **1**, 167–186 (1981).
52. B. Parthasarathy, N. A. Sontakke, A. A. Monot, D. R. Kothawale, Droughts/floods in the summer monsoon season over different meteorological subdivisions of India for the period 1871–1984. *J. Clim.* **7**, 57–70 (1987).
53. W. Huo, T. Yao, Y. Li, Increasing atmospheric pollution revealed by Pb record of a 7000 m ice core. *Chin. Sci. Bull.* **44**, 1309–1312 (1999).
54. K. Lee *et al.*, Isotopic signatures for natural versus anthropogenic Pb in high-altitude Mt. Everest ice cores during the past 800 years. *Sci. Total Environ.* **412–413**, 194–202 (2011).
55. Z. Li, T. Yao, L. Tian, B. Xu, Y. Li, Atmospheric Pb variations in Central Asia since 1955 from Muztagata ice core record, eastern Pamirs. *Chin. Sci. Bull.* **51**, 1996–2000 (2006).
56. E. Osterberg *et al.*, Ice core record of rising lead pollution in the North Pacific atmosphere. *Geophys. Res. Lett.* **35**, L05810 (2008).
57. J. M. Pacyna, E. G. Pacyna, An assessment of global and regional emissions of trace metals to the atmosphere from anthropogenic sources world-wide. *Environ. Rev.* **9**, 269–298 (2001).
58. C. Uglietti, P. Gabrielli, J. W. Olesik, A. Lutton, L. G. Thompson, Large variability of trace element mass fractions determined by ICP-SFMS in ice core samples from worldwide high altitude glaciers. *Appl. Geochem.* **47**, 109–121 (2014).
59. P. Gabrielli *et al.*, Early atmospheric contamination on the top of the Himalayas since the onset of the European Industrial Revolution. NOAA/World Data Service for Paleoclimatology. <https://www.ncdc.noaa.gov/paleo/study/28510>. Deposited 21 January 2020.